J. Plasma Physics (2012), *vol.* 78, *part* 4, *pp.* 497–500. © Cambridge University Press 2012
doi:10.1017/S0022377812000621

Energetic electron generation by magnetic reconnection in laboratory laser-plasma interactions

Q.-L. DONG[1,2], D.-W. YUAN[2], S.-J. WANG[2], Y. T. LI[2], X. LIU[2], S. E. JIANG[3], Y. K. DING[3], K. DU[3], M.-Y. YU[4,5], X.-T. HE[4,6], Y. J. TANG[3], J. Q. ZHU[7], G. ZHAO[8], Z.-M. SHENG[2,9] and J. ZHANG[2,9]

[1]School of Physics and Optoelectronic Engineering, Ludong University, Yantai 260405, China (qldong@aphy.iphy.ac.cn)
[2]Beijing National Laboratory of Condensed Matter Physics, Institute of Physics, Chinese Academy of Sciences, Beijing 100080, China
[3]Research Center for Laser Fusion, China Academy of Engineering Physics, Mianyang 621900, China
[4]Institute for Fusion Theory and Simulation, Physics Department, Zhejiang University, Hangzhou 310027, China (mmyu@zju.edu.cn)
[5]Institute for Theoretical Physics I, Ruhr University, D-44780 Bochum, Germany
[6]Institute of Applied Physics and Computational Mathematics, Beijing 100094, China
[7]National Laboratory on High Power Lasers and Physics, Shanghai 201800, China
[8]Key Laboratory of Optical Astronomy, National Astronomical Observatories, Chinese Academy of Sciences, Beijing 100012, China
[9]Key Laboratory for Laser Plasmas (MoE) and Department of Physics, Shanghai Jiao Tong University, Shanghai 200240, China (zmsheng@sjtu.edu.cn and jzhang1@sjtu.edu.cn)

(Received 30 October 2011; revised 30 May 2012; accepted 1 June 2012; first published online 6 July 2012)

Abstract. The magnetic reconnection (MR) configuration was constructed by using two approaching laser-produced plasma bubbles. The characteristics of the MR current sheet were investigated. The driving energy of the laser pulse affects the type of the current sheet. The experiments present "Y-type" and "X-type" current sheets for larger and smaller driving energy, respectively. The energetic electrons were found to be well-collimated. The formation and ejection of plasmoid from the "Y-type" current sheet was expected to enhance the number of accelerated electrons.

1. Introduction

Magnetic reconnection (MR) plays important roles in particle acceleration and heating in astrophysical and laboratory plasmas. For example, in solar flares and other related impulsive events, MR is accepted as a main cause; and energetic electrons between 10 keV and 100 keV produced during MR are found to carry half of the released energy in the process (Lin and Hudson 1970). MR is also responsible for the energetic particles generated from the Earth's magnetosphere (Øieroset et al. 2002; Wang et al. 2010), which is the reason for the dramatic auroral displays. At the same time, MR has also been found in other unmagnetized planets (Zhang et al. 2012). In laboratory, magnetic reconnection is under investigation in various devices such as the Swarthmore Spheromak Experiments (SSE) (Brown et al. 2002), the Madison Symmetric Torus (MST) (Magee et al. 2011), the Magnetic Reconnection Experiments (MRX) (Yamada et al. 2010), and tokamaks (Savrukhin 2001). Superthermal particles with power-law scaling at the high energy tail were observed in some of these experiments. In laser-plasmas, the magnetic reconnection can also play key roles in ion acceleration. Particle-in-cell (PIC) simulations of electromagnetic filament instability indicate that the magnetic reconnection process taking place during the filament coalescence will help to form a large quasi-static charge separation field by ejecting out local electrons (Sakai et al. 2002). In elaborately designed experiments with two approaching laser-plasma bubbles, bidirectional plasma jets were observed with magnetic field annihilation at the midplane between laser spots (Nilson et al. 2006; Li et al. 2007; Zhong et al. 2010), which was recognized as a magnetic reconnection process.

The electrons can be accelerated by a parallel electric field along separatrices in reconnections with guide fields (Pritchett and Coroniti 2004; Drake et al. 2005; Huang et al. 2010), or by the inductive electric field in the vicinity of the X-line, where electrons are first accelerated along the inductive electric field out of the MR plane, and then gyrated to the direction of the magnetic field along the direction of separatrices (Fu et al. 2006). The Fermi-type acceleration was also found in reconnection with magnetic islands formed as shown in recent PIC simulations (Drake et al. 2006). The inductive electric field formed at the two ends of the magnetic island because of island contraction was also supposed to be responsible for the large number of energetic electrons (Fu et al. 2006). Such theoretical predictions were verified by the spacecraft observation evidence of the

https://doi.org/10.1017/S0022377812000621 Published online by Cambridge University Press

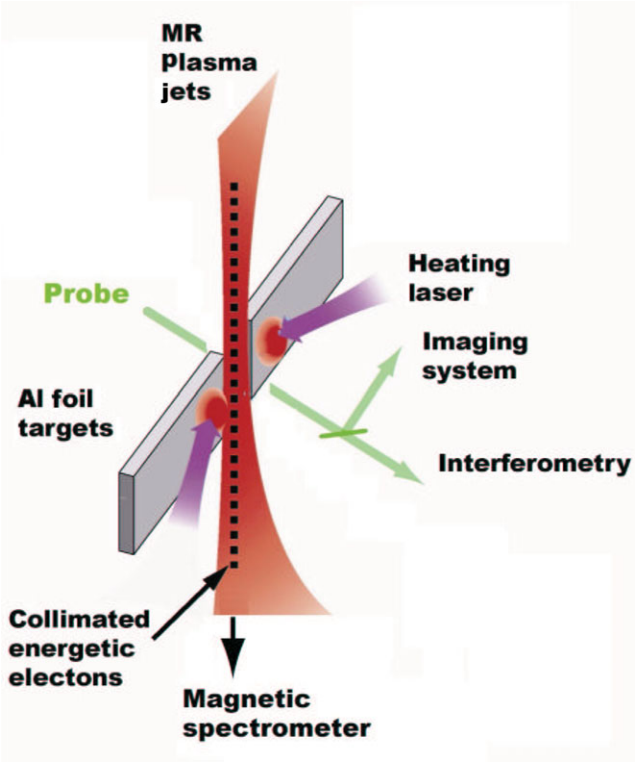


Figure 1. (Colour online) Experimental setup.

link between energetic electrons and magnetic islands in the Earth's magnetotail (Chen et al. 2008; Wang et al. 2010). Laboratory experiments were conducted on MST with observations of the anisotropic temperature distribution of impurity ions, which might indicate the existence of the electric field acceleration, and the power-law scaling at the high energy end of ion distribution, which is attributed to the magnetic islands formed as a resultof the close proximity of tearing mode resonant surfaces. However, the experimental results cannot give a conclusion about the right acceleration mechanism (Magee et al. 2011).

Here, in this paper, we present our experimental investigations of energetic electron generation by the MR process. It is suggested that the well-collimated energetic electrons are accelerated by the inductive electric field parallel along the MR separatrices. With a plasmoid formed, the electron distribution presents a power-law scaling at the high energy end, indicating the presence of the Fermi-type acceleration.

2. Experimental setup

The experiment was performed on the SG-II laser facility. The setup of experiments is illustrated schematically in Fig. 1. Four heater beams at a wavelength of 527 nm, shaped temporally with 0.9 ns flat-top and 0.1 ns ramp front and tail, respectively, were divided into two groups of equal energy of around 450 J, and focused by $F = 3$ optics simultaneously (within ± 25 ps) on two 50-μm-thick Al foil targets. The two Al foil

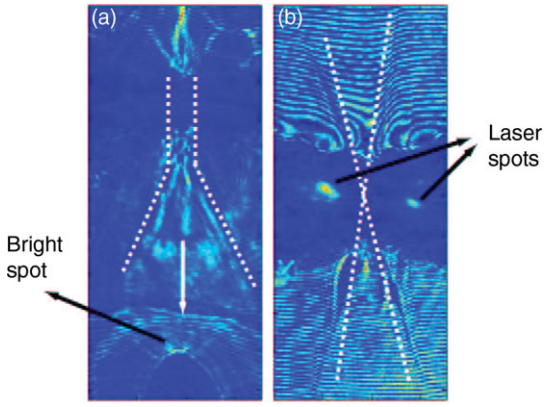


Figure 2. (Colour online) Interferometry images for different heating laser energy. (a) is the image of the current sheet with "Y-type" end for heating energy of 450 J on each laser spot; (b) is the image of the current sheet of "X-type" for heating energy of 350 J on each laser spot.

targets had sizes of 0.7 mm × 0.3 mm in the horizontal and vertical directions, respectively, and were separated from each other in horizontal direction by a gap of 150–240 μm. The two focal spots were measured to have diameters of less than 150 μm FWHM, giving an average laser intensity of the order of 10^{14}–10^{15} W cm^2. While the distance between two laser spots was variable, we focused on the situation with a laser-spot separation of 400 ± 25 μm. The diagnostic for the laser-plasma density profile was the modified Nomarski interferometer with the magnification of 3.5. The 9th beam of SG-II facility, centered at 527 nm in a Gaussian profile of 150 ps, was used as a probe propagating perpendicularly to the target surface at various delays with respect to four heater beams. To measure the distribution of energetic electrons produced by the expected magnetic reconnection, a magnetic spectrometer was installed 15 cm below the horizontal surface with the line connecting two laser foci. The axis of the incidence pinhole of the spectrometer is localized within the target surface, with a diameter of 3 mm producing an acceptance angle of 1.5°. The upper limit of the spectrometer is 2 MeV, and the energy resolution is $E/\delta E \sim 80$.

3. Experimental results and discussion

3.1. The morphology around the magnetic reconnection region

Figure 2 shows the interferometry images of the MR region. Figure 2(a) is the one taken for the shot with the heating energy of ~450 J on each laser spot, whereas Fig. 2(b) shows the one with the heating energy of ~350 J at each spot. It is obvious that with different heating energies on the laser spot, different kinds of MR regions are formed. Figure 2(a) shows the MR region of "double-Y" with the theoretically predicted three electron jets presented at the end of the current sheet. However, Fig. 2(b) shows typical "X-type" MR sites.

https://doi.org/10.1017/S0022377812000621 Published online by Cambridge University Press

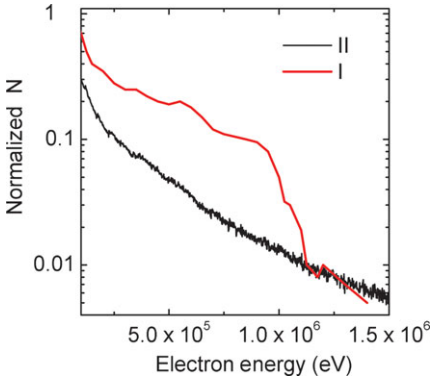


Figure 3. (Colour online) The electron energy distribution for two situations with different heating energies. I is for the situation with heating energy of 450 J on each laser spot; II is for the situation with heating energy of 350 J.

The formation of the "double-Y" region with higher energy is due to faster expansion of laser-plasma with the self-generated magnetic field, which causes the magnetic field to pile up while the reconnection is starting from the center to reduce the magnetic field, i.e. the MR in the higher energy laser-plasmas is a strongly driven case (Fox et al. 2011). The "double-Y" type current sheet is unstable, since the aspect ratio is large, and a plasmoid is formed and ejected out (Dong et al. 2012). It is interesting to point out that, although in both situations, the ejected plasmas form a fan-like region, the detailed structure is different. For the "double-Y" current sheet, it is worth pointing out that the three jet-like structures can be defined as the electron diffusion regions that consist of energetic electrons (Karimabadi et al. 2007; Shay et al. 2007). The bright spot in Fig. 2(a) is produced by energetic electrons colliding on a pre-set sample sphere, which is also an evidence of good collimation of electron beam.

3.2. *The produced energetic electron beam and its generation*

Figure 3 shows the directly measured electron energy distribution curves for two situations: (I) is for the shot with a "double-Y" current sheet, where a plasmoid is produced actually, and (II) is for the shot producing a typical "X-type" current sheet. It is obvious that with the plasmoid formation, the electron acceleration is much enhanced. Although the particle acceleration during MR still needs further investigation, here with the morphological feature of good collimation and the relativistic energy, the experimental results still shed light on the possible acceleration mechanism in present experiments.

According to the Fermi acceleration model, or the diffusive shock acceleration (DSA) model, the acceleration time of particles to energy of $E_{\max}$ is $\tau_{\rm acc} \sim 6.7\,\eta c\,E_{\max}/ZeBV_{\rm sk}^2$, where Ze is the particle charge, $V_{\rm sk}$ is the shock speed, and η is the parameter characterizing the efficiency of diffusion. For coronal plasmas, electrons need seconds or minutes to be accelerated to the energy of 0.1–10 MeV if taking $\eta \sim 1$–10^4, which is consistent with the observed flare time, indicating the dominance of Fermi acceleration in impulsive solar energetic electrons as discussed earlier (Drake et al. 2006; Chen et al. 2008). For the present laser-plasma system, however, electrons with energy in MeVs can only be achieved after tens of nanoseconds or microseconds if the DSA mechanism dominates the acceleration process even with the assumption of the Bohm diffusion as $\eta \sim 1$. Such acceleration time is much longer than the experimentally observed flare time of ~100 ps of the current sheet and two bright ridges. So rather than the Fermi-type mechanism, a much more efficient method is expected to explain the generation of energetic electrons in such a time scale. Numerical simulations have suggested that with the single X-line configuration such as in the present system, the electrons can be accelerated to ultrahigh energy by the reconnected electric field (Pritchett and Coroniti 2004; Drake et al. 2005; Huang et al. 2010). For electrons to attain energies as high as MeV in ~ 100 ps, the electric field should be $\sim 10^8$ V/m and an acceleration distance of ~ 1 cm. Such an electric field in the present system corresponds to the magnetic annihilation of tens of Tesla within 0.1 ns according to the Faraday law $\nabla \times \mathbf{E} = -\partial \mathbf{B}/\partial t$, indicating a reconnection rate of 0.1–0.3, which is consistent with the rate calculated by the measured magnetic exhaust wedge angle $\tan\theta_{\rm rec} \sim 0.25$–0.35. The large displacement is also possible but only if electrons exhibit behaviors of gyration in magnetic field, or re-entry in the electric field circularly due to reflection by the quasi-static magnetic fields. This is the right situation in the present experiments where the electric field of the MR diffusion region occupies only a small part of the whole magnetic topology, both of which in conjunction construct practically a cyclotron that accelerates electrons efficiently as observed in the experiments. Different from solar flare plasmas, here in the laser-plasma systems, electrons gain energy dominantly from the electric fields, rather than from multiple bouncing behavior between moving fronts and ends of plasmoids, i.e. the classical Fermi acceleration process.

4. Summary

In summary, by using two approaching laser-produced plasma bubbles, the magnetic reconnection scenario is constructed. Because of different driving energy applied, the morphology of the current sheets presents the "Y-type" and "X-type" characteristics, respectively. It is found that the energetic electron jet has a good collimation, which indicates that the electrons are mainly accelerated by the inductive electric field. But the comparison between the measured electron energy distributions from the two situations with different driving energy indicates that the formation of the plasmoid can help enhance the electron acceleration.

https://doi.org/10.1017/S0022377812000621 Published online by Cambridge University Press

Acknowledgements

This work is jointly supported by the National Natural Science Foundation of China (Grant nos. 10835003, 11074297, 11105217, and 10925421), the CAS project KJCX2-YWT01. We also thank the staff of the target manufacture group at Research Center for Laser Fusion, and the staff of the National Laboratory on High Power Lasers and Physics for their help in experiments.

References

Brown, M. R., Cothran, C. D., Landreman, M., Schlossberg, D., Matthaeus, W. H., Qin, G., Lukin, V. S. and Gray, T. 2002 Energetic particles from three-dimensional magnetic reconnection events in the Swarthmore Spheromak Experiment. *Phys. Plasmas* **9**, 2077–2084.

Chen, L. J., Bhattacharjee, A., Puhl-Quinn, P. A., Yang, H., Bessho, N., Imada, S., Muehlbachler, S., Daly, P. W., Lefebvre, B., Khotyaintsev, Y. et al. 2008 Observation of energetic electrons within magnetic islands. *Nat Phys.* **4**, 19–23.

Dong, Q. L., Wang, S. J., Lu, Q. M., Huang. C., Yuan, D. W., Liu, X., Lin, X. X., Li, Y. T., Wei, H. G., Zhong, J. Y. et al. 2012 Plasmoid ejection and secondary current sheet generation from magnetic reconnection in laser-plasma interaction. *Phys. Rev. Lett*. **108**, 215001.

Drake, J. F., Shay, M. A., Thongthai, W. and Swisdak, M. 2005 Production of energetic electrons during magnetic reconnection. *Phys. Rev. Lett*. **94**, 095001.

Drake, J. F., Swisdak, M., Che, H. and Shay, M. A. 2006 Electron acceleration from contracting magnetic islands during reconnection. *Nature* **443**, 553–556.

Fox, W., Bhattacharjee, A. and Germaschewski, K. 2011 Fast magnetic reconnection in laser-produced plasma bubbles. *Phys. Rev. Lett*. **106**, 215003.

Fu, X. R., Lu, Q. M. and Wang, S. 2006 The process of electron acceleration during collisionless magnetic reconnection. *Phys. Plasmas* **13**, 012309.

Huang, C., Lu, Q. and Wang, S. 2010 The mechanisms of electron acceleration in antiparallel and guide field magnetic reconnection. *Phys. Plasmas* **17**, 072306.

Karimabadi, H., Daughton, W. and Scudder, J. 2007 Multi-scale structure of the electron diffusion region. *J. Geophys. Res. Lett*. **3**4, L13104.

Li, C. K., Seguin, F. H., Frenje, J. A., Rygg, J. R., Petrasso, R. D., Town, R. P. J., Landen, O. L., Knauer, J. P. and Smalyuk, V. A. 2007 Observation of megagauss-field topology changes due to magnetic reconnection in laser-produced plasmas. *Phys. Rev. Lett*. **99**, 055001.

Lin, R. P. and Hudson, H. S. 1970 10-100 keV electron acceleration and emission from solar flares. *Solar Physics* **17**, 412–435.

Magee, R. M., Den Hartog, D. J., Kumar, S. T. A., Almagri, A. F., Chapman, B. E., Fiksel, G., Mirnov, V. V., Mezonlin, E. D. and Titus, J. B. 2011 Anisotropic ion heating and tail generation during tearing mode magnetic reconnection in a high-temperature plasma. *Phys. Rev. Lett*. **107**, 065005.

Nilson, P. M., Willingale, L., Kaluza, M. C., Kamperidis, C., Minardi, S., Wei, M. S., Fernandes, P., Notley, M., Bandyopadhyay, S., Sherlock, M. et al. 2006 Magnetic reconnection and plasma dynamics in two-beam laser-solid interactions. *Phys. Rev. Lett*. **97**, 255001.

Øieroset, M., Lin, R. P., Phan, T. D., Larson, D. E. and Bale, S. D. 2002 Evidence for electron acceleration up to ∼300 keV in the magnetic reconnection diffusion region of earth's magnetotail. *Phys. Rev. Lett*. **89**, 195001.

Pritchett, P. L. and Coroniti, F. V. 2004 Three-dimensional collisionless magnetic reconnection in the presence of a guide field. *J. Geophys. Res*. **109**, A01220.

Sakai, J., Saito, S., Mae, H., Farina, D., Lontano, M., Califano, F., Pegoraro, F. and Bulanov, S. V. 2002 Ion acceleration, magnetic field line reconnection, and multiple current filament coalescence of a relativistic electron beam in a plasma. *Phys. Plasmas* **9**, 2959–2970.

Savrukhin, P. V. 2001 Generation of suprathermal electrons during magnetic reconnection at the sawtooth crash and disruption instability in the T-10 Tokamak. *Phys. Rev. Lett*. **86**, 3036.

Shay, M. A., Drake, J. F. and Swisdak, M. 2007 Two-scale structure of the electron dissipation region during collisionless magnetic reconnection. *Phys. Rev. Lett*. **99**, 155002.

Wang, R. S., Lu, Q. M., Huang, C. and Wang, S. 2010 Multispacecraft observation of electron pitch angle distributions in magnetotail reconnection. *J. Geophys. Res*. **115**, A01209.

Yamada, M., Kulsrud, R. and Ji H. T. 2010 Magnetic reconnection. *Rev. Modern Phy*. **82**, 603.

Zhang, T. L., Lu, Q. M., Baumjohann, W., Russell, C. T., Fedorov, A., Barabash, S., Coates, A. J., Du, A. M., Cao, J. B. Nakamura, R., et al. 2012 Magnetic reconnection in the near Venusian magnetotail. *Sciences* **336**, 567.

Zhong, J., Li, Y. T., Wang, X. G., Wang, J. Q., Dong, Q. L., Xiao, C. J., Wang, S. J., Liu, X., Zhang, L., An, L. et al. 2010 Modelling loop-top X-ray source and reconnection outflows in solar flares with intense lasers. *Nat. Phys*. **6**, 984–987.

https://doi.org/10.1017/S0022377812000621 Published online by Cambridge University Press